

1 A thermodynamic approach to effective stresses  
2 in unsaturated soils incorporating the concept  
3 of partial pore deformations

4 Patrick Dangla<sup>a\*</sup>, Jean-Michel Pereira<sup>a</sup>

5 November 6, 2013

6 a: Université Paris-Est, Laboratoire Navier (UMR 8205), CNRS, ENPC,  
7 IFSTTAR, F-77420 Marne-la-Vallée

8 \* : Corresponding author

9 **Abstract**

10 The thermodynamical analysis presented here follows from the work  
11 of Coussy et al [13] who proposed a thermodynamically consistent model  
12 for unsaturated soils which is based on a Bishop-like effective stress to  
13 describe the stress-strain relationship while the water saturation (or the  
14 capillary pressure) is involved in a saturation-induced hardening in ad-  
15 dition to the mechanical hardening. We extended this model to include  
16 the effect of interfaces in the mechanical behaviour and we showed that  
17 the Bishop-like stresses involved in the elastic and plastic responses re-  
18 spectively can take different expressions. The Modified Cam-Clay model  
used for saturated soils is extended to unsaturated soils through the use of

19 these Bishop-like stresses. This model is compared to some experimental  
20 results reported from the literature.

21 Keywords: Unsaturated soil, Effective stress, Thermodynamics

## 22 **1 Introduction**

23 The concept of effective stress in unsaturated soils goes back to the work of  
24 Bishop [4] who extended the concept of Terzaghi's effective stress by introducing  
25 a weighted average of gas and liquid pressures [5, 7]. This proposal encountered  
26 difficulties in explaining collapse behaviour [6, 9, 1, 23]. Then many authors  
27 have pointed out the need of two independent stress state variables to account  
28 for experimental observations on the mechanical behavior of unsaturated soils  
29 [18]. On that basis elastoplastic models were formulated [2, 20]. These models  
30 can be viewed as an extension of the Cam-Clay model to unsaturated situations.  
31 This has launched the development of many other models [24, 30, 7, 28, 29, 19,  
32 36, 34, 15, 33]. All these models are founded on two independent stresses even  
33 though they vary widely in the choice of the stresses. Some of them [32] chose to  
34 refer one stress to a Bishop-type stress. But all those models require the suction  
35 or the capillary pressure as an additional and independent stress. [The reader](#)  
36 [can refer to the comprehensive review of effective stresses proposed by Nuth et](#)  
37 [al \[31\]](#). In most of these models suction is a hardening variable and thus has a  
38 status somehow different from the Bishop stress. As noted by Coussy [13, 12]  
39 the status of the suction or capillary pressure is two fold. Its variations control

40 the fluid invasion process through the retention curve and they also control the  
41 mechanical behaviour through the deformation of the pores they induced. This  
42 can be a source of confusion in the formulation of the constitutive equations  
43 as pointed out by Alonso et al [3]. A significant breakthrough in the way of  
44 clarification, was achieved by Coussy [12] who proposed a more appropriate  
45 definition of the saturation degree, called Lagrangian saturation degree. This  
46 new definition is only associated to the invasion process, i.e to the creation  
47 and destruction of fluid-solid interface areas during wetting-drying processes.  
48 In contrast this saturation degree is not affected by the deformation process of  
49 the porous network. Thanks to this new concept Coussy et al [13] have given  
50 a physical background to the coefficient involved in the Bishop effective stress  
51 and proposed, on this physical basis, an extension of the Cam-Clay model to  
52 unsaturated conditions which is thermodynamically consistent. Experimental  
53 data on shear strength suggest that this Bishop coefficient is mostly smaller than  
54 the saturation degree generally used in the expression of the Bishop effective  
55 stress [3].

56 Following the approach of Coussy, we explore here the effect of the interface  
57 energy on the mechanical behaviour of unsaturated soils which was neglected  
58 in the work of Coussy [11, 13]. [As opposed to what was done in Coussy, the](#)  
59 [interface energy here depends on the deformation of the material.](#) We also derive  
60 two Bishop-like effective stresses related to the elastic and plastic responses  
61 respectively. Finally we propose a simple extension of the Modified Cam-Clay  
62 model to unsaturated conditions and some comparisons with experimental data

63 are shown.

64 An unsaturated soil consists in a solid skeleton composed of solid grains in  
65 contact, a gas phase and a liquid phase. These three phases interact with each  
66 other through interfaces which sustain surface stress and possess their own en-  
67 ergy. These interfaces play a fundamental role in the thermodynamic analysis of  
68 unsaturated soils. Accordingly the thermodynamics of a representative volume  
69 element of unsaturated soil can be addressed by considering three different sys-  
70 tems. The first one is the soil itself, as depicted above, including all the matter  
71 in all form contained in the RVE. It is an open thermodynamic system exchang-  
72 ing gas and liquid mass. The second system is obtained by removing the bulk  
73 fluid masses whatever the fluid form. It is then formed of the solid phase and  
74 the interfaces only. This system is still subjected to the gas and liquid pressures  
75 through the interfaces. However these pressure are considered now as external  
76 forces. Like Coussy [13] we'll call this system the "apparent solid skeleton"  
77 (subscript "ske") since it includes interfaces with energy concentrated on those  
78 surfaces. By removing the interfaces we can obtain a third system consisting  
79 in only the solid phase. We will call it the "solid matrix" (subscript "sol") in  
80 the following. This system is now subjected to external forces which differ from  
81 the gas and liquid pressures since part of these pressures are absorbed by the  
82 interface surface stresses. We will assume that these forces can be represented  
83 by two effective pressures exerted on the part of the solid wall in contact with  
84 the solid-liquid and solid-gas interfaces. We will denote them by  $\pi_L$  and  $\pi_G$ .  
85 We must note that such effective pressures have already been derived formally

86 by other authors from a microscopical approach and by making use of averaging  
 87 technics [21, 22].

## 88 **2 Effective pore pressures and interface energy**

89 Consider a volume  $V_0$  of soil in its undeformed reference configuration. In the  
 90 current configuration the volume is  $V$ , the pore volume is  $\phi V_0$  where  $\phi$  is the  
 91 Lagrangian porosity [11]. The pore volume occupied by the liquid and gas phase  
 92 are given by  $\phi_L V_0$  and  $\phi_G V_0$ , where the  $\phi_J$  ( $J = L, G$ ) can be coined as partial  
 93 Lagrangian porosities respectively. Furthermore we have  $\phi_L + \phi_G = \phi$ .

94 The balance free energy of the apparent solid skeleton, at constant temper-  
 95 ature, can be expressed as [13]

$$dF_{\text{ske}} = \sigma_{ij} d\epsilon_{ij} + p_L d\phi_L + p_G d\phi_G \quad (1)$$

96 The current partial porosity  $\phi_J$  can be written in the form [12]

$$\phi_J = \phi_0 S_J + \varphi_J ; \quad S_L + S_G = 1 \quad (2)$$

97 where  $S_J$  is the Lagrangian saturation degree and  $\varphi_J$  is the deformation of the  
 98 porous network occupied by the phase J which can be coined as the partial  
 99 pore deformation. In Eq. (2)  $\phi_0 S_J$  is the volume occupied by the fluid J prior  
 100 to any deformation i.e. by the part of the porous volume of the undeformed  
 101 reference configuration which is delimited by the internal solid walls wetted by  
 102 the fluid J [12]. The variations of  $S_J$  is therefore associated to the invasion  
 103 process of interfaces i.e. to the displacement of the common line between the

104 three interfaces onto the solid surface. Substituting expression (2) for  $\phi_J$  in (1)  
 105 reads

$$dF_{\text{ske}} = \sigma_{ij}d\epsilon_{ij} + p_L d\varphi_L + p_G d\varphi_G - \phi_0(p_G - p_L)dS_L \quad (3)$$

106 The three first terms of the right hand side of Eq. (3) represent the defor-  
 107 mation work undergone by the apparent solid skeleton while the fourth term  
 108 is the energy supply to create new or suppress existing inner interfaces. As a  
 109 consequence the energy of the solid skeleton can be split in two parts:

$$F_{\text{ske}} = F_{\text{sol}}(\epsilon_{ij}, \varphi_L, \varphi_G, S_L) + F_{\text{int}}(\varphi_L, \varphi_G, S_L) \quad (4)$$

110 where  $F_{\text{sol}}$  is the free energy stored in the solid matrix and  $F_{\text{int}}$  is the free energy  
 111 of interfaces. The free energy of the solid matrix,  $F_{\text{sol}}$ , is mainly a function of  
 112 the deformation variables  $\epsilon_{ij}, \varphi_L, \varphi_G$  with  $S_L$  intervening as a coupling term.  
 113 In this sense the derivative  $\frac{\partial F_{\text{sol}}}{\partial S_L}$  will always be coupled with the deformation  
 114 variables and therefore will be considered as a small term compared to  $\frac{\partial F_{\text{int}}}{\partial S_L}$ .  
 115 Similarly  $F_{\text{int}}$  depends essentially on  $S_L$  and the partial deformation of pores,  
 116  $\varphi_L$  and  $\varphi_G$ , as coupling terms. Because interfaces are located in the porosity,  
 117  $F_{\text{int}}$  is assumed as independent of the skeleton strains.

118 According to Eq. (3) the force-like vector formed by the stress tensor, the  
 119 fluid pressures and the pressure difference  $-\phi_0(p_G - p_L)$  is energy conjugate  
 120 to the deformation-like vector formed by the strain tensor, the partial pore  
 121 deformations and the saturation degree. As already noted by Coussy et al  
 122 [13]: "In the familiar capillary case, although the suction can be defined as  
 123 the difference between the pressures of the non-wetting and wetting phases, the

124 various role of the pressure difference must be well separated from that of the  
 125 suction". Indeed the status of fluid pressures in the energy change is two fold.  
 126 On one hand the mechanical pressures that are exerted on complementary parts  
 127 of the solid wall from the liquid and gas, govern the process of deformation of the  
 128 material. The saturation degree which controls the partition of these pressures  
 129 on the solid wall can be considered as an independent parameter of the behaviour  
 130 and therefore decoupled from these mechanical pressures. On the other hand the  
 131 process of invasion, linked to the change of saturation degree, is controlled by  
 132 the suction through the retention curve. Even though the suction is eventually  
 133 given by the difference between the gas and liquid pressures, the status of the  
 134 suction is here well separated from that of the mechanical pressures.

135 From a thermodynamical point of view these different status of fluid pres-  
 136 sures form three independant forces which are energy conjugate to the three  
 137 independent thermodynamical variables:  $\varphi_L, \varphi_G, S_L$ .

## 138 2.1 Energy of the solid matrix

139 Combining (3) and (4), the free energy of the sole solid matrix satisfies

$$(dF_{\text{sol}})_{S_L} = \sigma_{ij} d\epsilon_{ij} + \pi_L d\varphi_L + \pi_G d\varphi_G \quad (5)$$

140 where

$$\pi_J = p_J - \left( \frac{\partial F_{\text{int}}}{\partial \varphi_J} \right)_{S_L, \varphi_K \neq J} \quad (6)$$

141 The interpretation of the effective pressure  $\pi_J$  can be addressed equivalently  
 142 as follows:

143 (i)  $\pi_J d\varphi_J$  is the infinitesimal deformation work given to the solid matrix  
 144 through the partial pore deformation  $d\varphi_J$ .

145 (ii)  $\pi_J$  represents, at the macroscopic scale, the modeling of the actual normal  
 146 stress exerted to the solid matrix. Therefore  $\pi_J$  can be coined as an  
 147 effective pore pressure.

148 (iii)  $p_J - \pi_J = \frac{\partial F_{\text{int}}}{\partial \varphi_J}$  is due to the surface tension sustained by the solid-fluid  
 149 interface and can be compared with the Young-Laplace equation<sup>1</sup>.

150 From the balance energy (5) the state laws read

$$\sigma_{ij} = \left( \frac{\partial F_{\text{sol}}}{\partial \epsilon_{ij}} \right)_{S_L, \varphi_J} \quad \pi_J = \left( \frac{\partial F_{\text{sol}}}{\partial \varphi_J} \right)_{S_L, \epsilon_{ij}, \varphi_{K \neq J}} \quad (7)$$

151 At constant saturation degree  $S_L$ , the linearization of the state laws (7) can pro-  
 152 vide a first approach of the constitutive equations of unsaturated soils. However  
 153 the coefficients involved in the linearization process must depend on  $S_L$ . As a  
 154 general rule the variable  $S_L$  appearing in the arguments of  $F_{\text{sol}}$  should be con-  
 155 sidered as a coupling term only. As a consequence expression for  $F_{\text{sol}}$  should  
 156 involve only small terms as strains and partial pore deformations:  $\epsilon_{ij}, \varphi_J$ .

157 On the other way, a general requirement for  $F_{\text{sol}}$  can be expressed as follows.  
 158 Along any loading path characterized by  $\pi_L = \pi_G$  the solid wall is subjected to  
 159 a uniform pore pressure. In that case, according to Eq. (5), we could expect  
 160 an expression for  $F_{\text{sol}}$  which is independent of  $S_L$  as long as  $\pi_L = \pi_G$ . In other

---

<sup>1</sup>In case of a spherical pore of radius  $r$ , it is easy to show that  $\frac{\partial F_{\text{int}}}{\partial \varphi_J} = \frac{2\gamma}{r}$  where  $\gamma$  is the surface tension



161 words the derivative  $\frac{\partial F_{\text{sol}}}{\partial S_L}$  should vanish for any value  $\pi_L = \pi_G$ :

$$\left( \frac{\partial F_{\text{sol}}}{\partial S_L} \right)_{\epsilon_{ij}, \varphi_K} = 0 \quad \forall \pi_L = \pi_G \quad (8)$$

## 162 2.2 Energy of interfaces

163 The interface free energy can be derived from the surface tension,  $\gamma_{IJ}$ , and the  
164 surface area,  $\omega_{IJ}$ , of the three interfaces according to

$$F_{\text{int}} = \gamma_{\text{SL}}\omega_{\text{SL}} + \gamma_{\text{SG}}\omega_{\text{SG}} + \gamma_{\text{GL}}\omega_{\text{GL}} \quad (9)$$

165 Since the previous approach has postulated that, at the macroscopic scale, this  
166 energy only depends on the 3 thermodynamical variables,  $(\varphi_L, \varphi_G, S_L)$ , such an  
167 expression must be consistent with expression (9) for any deformation process.  
168 To go further we are going to make some reasonable assumptions for interface  
169 energy. Surface tensions are assumed constant or only temperature dependent.  
170 Accordingly since interface energy is spread over surfaces we can assume the  
171 following property regarding the dependence of  $F_{\text{int}}$  upon the partial pore de-  
172 formations:

$$F_{\text{int}}(\varphi_L + \lambda\phi_0 S_L, \varphi_G + \lambda\phi_0 S_G, S_L) = \left(1 + \frac{2}{3}\lambda\right) F_{\text{int}}(\varphi_L, \varphi_G, S_L) \quad \forall \lambda \ll 1 \quad (10)$$

173 Statement (10) expresses that the interface energy change, at constant satura-  
174 tion, is only due to the change of the surface areas of pores in the process of  
175 deformation. Indeed from the current state any virtual (small) homogeneous  
176 dilation of coefficient  $(1 + \frac{1}{3}\lambda)$  would cause an increase of volume by a factor  
177  $(1 + \lambda)$  (i.e the volume of pore  $\phi_0 S_J$  would increase by  $\lambda\phi_0 S_J$ ) and an increase of  
178 surface by a factor  $(1 + \frac{2}{3}\lambda)$ . Property (10) implicitly assumes that the surface

179 stresses don't depend on the solid surface strains and coincide with the surface  
 180 tensions,  $\gamma_{\text{LJ}}$ , thereby assuming that they are constant. Derivation with respect  
 181 to  $\lambda$  entails

$$\phi_0 S_{\text{L}} \left( \frac{\partial F_{\text{int}}}{\partial \varphi_{\text{L}}} \right)_{\epsilon_{ij}, \varphi_{\text{G}}} + \phi_0 S_{\text{G}} \left( \frac{\partial F_{\text{int}}}{\partial \varphi_{\text{G}}} \right)_{\epsilon_{ij}, \varphi_{\text{L}}} = \frac{2}{3} F_{\text{int}} \quad (11)$$

182 Finally linearizing  $F_{\text{int}}$  with respect to the partial pore deformations  $\varphi_{\text{J}}$  gives

$$F_{\text{int}} = \frac{2}{3} U_{\text{L}}(S_{\text{L}}) \varphi_{\text{L}} + \frac{2}{3} U_{\text{G}}(S_{\text{L}}) \varphi_{\text{G}} + \phi_0 U(S_{\text{L}}) \quad (12)$$

183 where  $U$  is the interface energy per unit of porous space prior to any deformation  
 184 process. Combining (11) and (12) shows that  $U$  is expressed as

$$U = S_{\text{L}} U_{\text{L}} + S_{\text{G}} U_{\text{G}} \quad (13)$$

185 where  $U_{\text{L}}$  and  $U_{\text{G}}$  are two interface energies associated to the liquid and gas  
 186 phases. From (6) we have

$$\pi_{\text{J}} = p_{\text{J}} - \frac{2}{3} U_{\text{J}} \quad (14)$$

187 With the help of the equations derived above the interface energy balance writes

$$dF_{\text{int}} = (p_{\text{L}} - \pi_{\text{L}}) d\varphi_{\text{L}} + (p_{\text{G}} - \pi_{\text{G}}) d\varphi_{\text{G}} - \left( \phi_0 (p_{\text{G}} - p_{\text{L}}) + \frac{\partial F_{\text{sol}}}{\partial S_{\text{L}}} \right) dS_{\text{L}} \quad (15)$$

188 Neglecting  $\frac{\partial F_{\text{sol}}}{\partial S_{\text{L}}}$  compared to  $\frac{\partial F_{\text{int}}}{\partial S_{\text{L}}}$ , the state laws of interface now read at the  
 189 first order

$$p_{\text{G}} - p_{\text{L}} = -\frac{dU}{dS_{\text{L}}} ; \quad p_{\text{L}} - \pi_{\text{L}} = \frac{2}{3} U_{\text{L}} ; \quad p_{\text{G}} - \pi_{\text{G}} = \frac{2}{3} U_{\text{G}} \quad (16)$$

190 These 3 state laws can be compared, in some way, with a kind of macroscopic  
 191 Young-Laplace law. The first law (16a) is the well known capillary or retention

192 cure. The two other laws (16b,16c) are unusual and difficult to apply because it  
 193 is not possible to measure energies  $U_J$  separately. One possible way to overcome  
 194 this difficulty comes from an exploitation of the microscopic definition of the  
 195 interface energy (9) which can be written, in the undeformed state and using  
 196 the Young equation, as

$$\phi_0 U = \gamma_{\text{SL}} \left( \omega_{\text{SL}} - \frac{\omega_{\text{GL}}}{\cos \theta} \right) + \gamma_{\text{SG}} \left( \omega_{\text{SG}} + \frac{\omega_{\text{GL}}}{\cos \theta} \right) \quad (17)$$

197 where  $\theta$  is the contact angle of the liquid assumed as the wetting phase. Then  
 198 we assume that each term of the rhs of Eq. (17) can be identified to that of  
 199 the rhs of Eq. (13). Using the property that the sum  $\omega_{\text{SL}} + \omega_{\text{SG}}$  is the total  
 200 surface of the solid wall (and therefore is constant), we can derive an expression  
 201 of  $S_J U_J$  in the form

$$S_{\text{L}} U_{\text{L}} = U(1) - \frac{\gamma_{\text{SL}}}{\gamma_{\text{SG}} - \gamma_{\text{SL}}} (U(S_{\text{L}}) - U(1)) \quad (18)$$

$$S_{\text{G}} U_{\text{G}} = \frac{\gamma_{\text{SG}}}{\gamma_{\text{SG}} - \gamma_{\text{SL}}} (U(S_{\text{L}}) - U(1)) \quad (19)$$

202 where  $U(1)$  can be set to 0 by considering the saturated state as a reference state.  
 203 Since liquid is the wetting phase the fraction  $\frac{\gamma_{\text{SL}}}{\gamma_{\text{SG}} - \gamma_{\text{SL}}}$  is a positive number that  
 204 we will denote by  $a$ , in the following, so that

$$S_{\text{L}} U_{\text{L}} = -a U(S_{\text{L}}) ; \quad S_{\text{G}} U_{\text{G}} = (1 + a) U(S_{\text{L}}) \quad (20)$$

205 We have to point out that the identification (20) relies on the assumption, albeit  
 206 natural, that the rhs of (17) and (13) can be identified term by term. Moreover  
 207 because the surface tensions  $\gamma_{\text{SJ}}$  are generally not known, the coefficient  $a$  should  
 208 be calibrated directly at the macroscopic scale.

### 209 **3 The Equivalent Pore Pressure model**

210 To derive this model, we will assume that along any loading path defined by a  
 211 constant saturation degree,  $dS_L = 0$ , and constant effective pressures,  $d\pi_J = 0$ ,  
 212 the partial pore deformation increment,  $d\varphi_J$  is a saturation dependent fraction  
 213 of the total pore deformation:

$$(d\varphi_L)_{S_L, \pi_J} = \chi d\varphi ; \quad (d\varphi_G)_{S_L, \pi_J} = (1 - \chi)d\varphi \quad (21)$$

214 where  $\chi$  is a saturation dependent factor that varies between 1, under saturated  
 215 state, and 0 under dried state. The choice  $\chi = S_L$  corresponds to the iso-  
 216 deformation assumption of the two partial pore volumes:  $\frac{d\varphi_L}{\phi_0 S_L} = \frac{d\varphi_G}{\phi_0 S_G}$  which  
 217 has to be satisfied whatever the saturation. Accordingly, when  $\chi = S_L$ , the  
 218 porous network is assumed to deform homogeneously whenever no pressure is  
 219 applied on the solid wall. This assumption is often used for convenient reasons  
 220 [11, 27, 10].

221 Integration of (21) gives

$$\varphi_L = \chi\varphi + \delta ; \quad \varphi_G = (1 - \chi)\varphi - \delta \quad (22)$$

222 where  $\delta$  is a function of  $(S_L, \pi_L, \pi_G)$  that must vanish under saturated and dried  
 223 states:

$$\delta(0, \pi_L, \pi_G) = \delta(1, \pi_L, \pi_G) = 0 \quad (23)$$

224 Incorporating expression (22) for  $\varphi_J$  in (5) gives

$$(dF_{\text{sol}})_{S_L} = \sigma_{ij} d\epsilon_{ij} + \pi d\varphi + \Delta d\delta \quad (24)$$

225 where we defined  $\pi$  and  $\Delta$  as follows

$$\pi = \chi\pi_L + (1 - \chi)\pi_G \quad (25)$$

$$\Delta = \pi_L - \pi_G \quad (26)$$

226 Defining the Legendre-Fenchel transform  $F_{\text{sol}}^* = F_{\text{sol}} - \sigma_{ij}\epsilon_{ij} - \pi\varphi - \Delta\delta$  entails

$$(dF_{\text{sol}}^*)_{S_L} = -\epsilon_{ij}d\sigma_{ij} - \varphi d\pi - \delta d\Delta \quad (27)$$

227 Since  $\delta$  only depends on  $(S_L, \pi, \Delta)$ , the integration of the state equation

$$\delta(S_L, \pi, \Delta) = - \left( \frac{\partial F_{\text{sol}}^*}{\partial \Delta} \right)_{S_L, \sigma_{ij}, \pi} \quad (28)$$

228 shows that  $F_{\text{sol}}^*$  can be split as follows

$$F_{\text{sol}}^* = F_{\text{sol}}^{*1}(\sigma_{ij}, \pi, S_L) - \int_0^\Delta \delta(S_L, \pi, u) du \quad (29)$$

229 Eq. (29) suggests that  $F_{\text{sol}}^{*1}$  can depend on  $S_L$ . Actually it cannot because of

230 the general requirement (8)<sup>2</sup>. Indeed injecting equality  $\Delta = 0$  in (29) and using

231 the property (8) show that  $S_L$  is decoupled from the stresses  $\sigma_{ij}$  and  $\pi$ . Thus

232  $F_{\text{sol}}^{*1}$  only depends on  $(\sigma_{ij}, \pi)$  with

$$dF_{\text{sol}}^{*1} = -\epsilon_{ij}d\sigma_{ij} - \varphi^* d\pi \quad (30)$$

233 where we defined

$$\varphi^* = \varphi - \int_0^\Delta \frac{\partial \delta}{\partial \pi}(S_L, \pi, u) du \quad (31)$$

234 Expression (31) for  $\varphi^*$  can be transformed by using the Maxwell symmetry

235 relation derived from (27)

$$\left( \frac{\partial \delta}{\partial \pi} \right)_{S_L, \Delta} = \left( \frac{\partial \varphi}{\partial \Delta} \right)_{S_L, \sigma_{ij}, \pi} \quad (32)$$

---

<sup>2</sup>where we can notice that  $\left( \frac{\partial F_{\text{sol}}}{\partial S_L} \right)_{\epsilon_{ij}, \varphi, \delta} = \left( \frac{\partial F_{\text{sol}}^*}{\partial S_L} \right)_{\sigma_{ij}, \pi, \Delta}$

236 We obtained

$$\varphi^* = \varphi|_{\Delta=0} \quad (33)$$

237 Hence  $\varphi^*$  turns out to be the total pore deformation that would have resulted  
 238 from  $\Delta = 0$ , i.e.  $\pi_L = \pi_G$ , while keeping the other variables as constant.

239 Therefore expression  $F_{\text{sol}}^{*1}(\sigma_{ij}, \pi)$  which is independent of  $S_L$ , must have the  
 240 same expression as that found under saturated state. The state equations

$$\epsilon_{ij} = - \left( \frac{\partial F_{\text{sol}}^{*1}}{\partial \sigma_{ij}} \right)_{\pi} \quad \varphi^* = - \left( \frac{\partial F_{\text{sol}}^{*1}}{\partial \pi} \right)_{\sigma_{ij}} \quad (34)$$

241 show that  $\pi$  play the role of an equivalent pore pressure in the sense that it  
 242 would be the pressure to apply to the liquid phase of the porous material under  
 243 saturated state, to get the same strains as those obtained under unsaturated  
 244 state, at the given stress state  $\sigma_{ij}$ . Note however that the total pore deforma-  
 245 tion that would be obtained under saturated state is  $\varphi^*$  and not that of the  
 246 unsaturated state,  $\varphi$ .

247 Assuming that, at the microscopic scale, the solid matrix is isotropic and  
 248 behaves elastically, with a compressibility constant  $k_s$ , an incremental loading  
 249 defined, at constant saturation degree, by  $d\sigma = -d\pi_L = -d\pi_G = -d\pi$ , will load  
 250 the solid grains by a uniform increment of pressure leading to a response given  
 251 by  $d\epsilon_{ii} = d\varphi/\phi_0 = d\varphi_J/(\phi_0 S_J) = -d\pi/k_s$ . Incorporating these last equations  
 252 into the general equation (22) leads to

$$\left( \frac{\partial \delta}{\partial \pi} \right)_{S_L, \Delta} = \left( \frac{\partial \varphi}{\partial \Delta} \right)_{S_L, \sigma_{ij}, \pi} = \frac{\phi_0(\chi - S_L)}{k_s} \quad (35)$$

253 showing that  $\delta$  and  $\varphi$  vary linearly with  $\pi$  and  $\Delta$ , respectively. Accordingly we

254 obtain for  $\varphi$

$$\varphi = \varphi^* + \frac{\phi_0(\chi - S_L)}{k_s} \Delta \quad (36)$$

255 showing that  $\varphi^* = \varphi$  in the iso-deformation assumption,  $\chi = S_L$ .

256 Furthermore the  $\delta$ - $\Delta$  relationship is expected to involve the elastic shear  
 257 property of the solid matrix. If we assume the linearity of such behavior we end  
 258 up with

$$\delta = \frac{\phi_0(\chi - S_L)}{k_s} \pi + \frac{\Delta}{g(S_L)} \quad (37)$$

259 where  $g(S_L)$  stands for an elastic modulus characterizing the elastic shear prop-  
 260 erty of the solid matrix.

261 When the solid grains are incompressible,  $k_s$  can be set to  $\infty$  in the previous  
 262 equations. The volumetric deformation of the soil is then equal to the total pore  
 263 deformation,  $\epsilon_v = \varphi = \varphi^*$ , and the balance (30) turns into

$$dF_{\text{sol}}^{*1} = -\epsilon_v d(\sigma + \pi) - \epsilon_q dq \quad (38)$$

264 where  $q$  and  $\epsilon_q$  are the deviatoric stress and strain respectively. From (38)

$$\epsilon_v = - \left( \frac{\partial F_{\text{sol}}^{*1}}{\partial(\sigma + \pi)} \right)_q \quad (39)$$

## 265 4 Elastic behavior

266 Under isotropic loading, the mechanical response of saturated soils is well de-  
 267 scribed by a constant compressibility coefficient,  $\kappa$ , in the form

$$de = -\kappa \frac{d(\sigma + p)}{\sigma + p} \quad (40)$$

268 where  $e$  stands for the void ratio. This coefficient has been measured on FoCa  
 269 clay used for engineered barrier [14]. The compression test is shown in the  
 270 figure (1) where only the BC lines are associated with the elastic response. The  
 271 compressibility coefficient is  $\kappa = 0.0977$ .

272 Since energy  $F_{\text{sol}}^1$  has been found to be independent of the saturation degree,  
 273 a comparison of (40) and (39) implies the general constitutive relationship

$$de = -\kappa \frac{d(\sigma + \pi)}{\sigma + \pi} \quad (41)$$

274 which should be valid for unsaturated situations and along any loading paths  
 275 and with the same constant compressibility coefficient as that involved in (40).  
 276 However to be able to apply the previous relation, the equivalent pore pressure,  
 277  $\pi$ , has to be computed from (25). This can be done from the water retention  
 278 curve of the material. This curve has been measured, at 20 and 80 °C, on the  
 279 same FoCa clay using the saturated salt solution technique upon imbibition path  
 280 [14]. This curve is shown in the figure (2a). During these tests no stress was  
 281 applied thereby, neglecting the atmospheric pressure,  $\sigma = 0$ . In these conditions  
 282 Eq. (41) turns into

$$de = -\kappa \frac{d\pi}{\pi} \quad (42)$$

283 The free swelling of these samples was measured and reported in figure (2b) in  
 284 terms of  $\pi$  calculated with the help of the measured retention curves, the gas  
 285 pressure being neglecting. We assume here the iso-deformation of pores, i.e.  
 286  $\chi = S_L$ . The reported measured points are found to be accurately lined up with  
 287 a slope  $\kappa = 0.0978$ , namely very close to that found in the previous experiment.



## 288 5 Plastic Modeling

289 We will assume in the following that irreversibility only affects the mechanical  
 290 behavior. Hysteresis of the retention curve will not be addressed here. As a con-  
 291 sequence, in non reversible transformation, the two first laws of thermodynamics  
 292 applied to the system composed of the solid matrix, gives the Clausius-Duhem  
 293 inequality in the form [11]

$$\sigma_{ij}d\epsilon_{ij} + \pi_L d\varphi_L + \pi_G d\varphi_G - (dF_{\text{sol}})_{S_L} \geq 0 \quad (43)$$

294 where now the free energy of the solid matrix,  $F_{\text{sol}}$ , must be argued by the  
 295 elastic part of the deformation variables and by hardening variables. Following  
 296 [13] this energy is split into two parts: (i) the elastic energy,  $W$ , stored in the  
 297 solid matrix which is the energy recoverable by a reversible mechanical process  
 298 and (ii) the locked energy,  $Z$ , which is the additional (not recoverable) part  
 299 of the elastic energy locked when irreversible mechanical processes have taken  
 300 place. For the sake of simplicity, the locked energy is assumed to depend on a  
 301 unique hardening variable,  $\alpha$ . Denoting with superscripts  $e$  and  $p$  the elastic  
 302 and plastic part of the deformation variables, respectively, we write

$$F_{\text{sol}} = W(\epsilon_{ij}^e, \varphi_L^e, \varphi_G^e, S_L) + Z(S_L, \alpha) \quad (44)$$

303 The state equations (7) being always valid provided that each deformation vari-  
 304 able be replaced by its elastic part, the use of expression (44) for  $F_{\text{sol}}$  in (43)  
 305 allows to write the Clausius-Duhem inequality as

$$\sigma_{ij}d\epsilon_{ij}^p + \pi_L d\varphi_L^p + \pi_G d\varphi_G^p + \beta d\alpha \geq 0 \quad (45)$$

306 where  $\beta$  is defined by

$$\beta = - \left( \frac{\partial Z}{\partial \alpha} \right)_{S_L} \quad (46)$$

307 The variable  $\beta$  is the hardening force as energy conjugate to the hardening  
 308 variable  $\alpha$ . It will be associated to the current limit of the elastic domain  
 309 defined by

$$f(\sigma, \pi_L, \pi_G, \beta) \leq 0 \quad (47)$$

310 Following the work of Coussy [13], to go further towards an effective stress, we  
 311 will assume that part of the flow rule is given by

$$(d\varphi_L^p)_{S_L} = \chi^p d\varphi^p ; \quad (d\varphi_G^p)_{S_L} = (1 - \chi^p) d\varphi^p \quad (48)$$

312 where  $\chi^p$  is a weighting factor ranging from 0 to 1. This factor is, a priori,  
 313 different from  $\chi$  which was introduced previously to describe the elastic response.  
 314 Similarly to what was done for  $\chi$ , we will assume that this factor depends  
 315 on the saturation degree:  $\chi^p(S_L)$ . The plastic incompressibility of the solid  
 316 grains is now introduced leading to  $\epsilon_v^p = \varphi^p$ . From the plastic incompressibility  
 317 assumption and (48) the dissipation (45) turns into

$$\sigma^B d\epsilon_v^p + q d\epsilon_q^p + \beta d\alpha \geq 0 \quad (49)$$

318 where  $\sigma^B$  is a Bishop-like stress defined by

$$\sigma^B = \sigma + \chi^p \pi_L + (1 - \chi^p) \pi_G \quad (50)$$

319 According to (50) and (49) the current elastic domain can be defined by

$$f(\sigma^B, q, \beta) \leq 0 \quad (51)$$

320 The flow rule is then expressed in the form

$$d\epsilon_v^p = d\lambda \left( \frac{\partial f}{\partial \sigma^B} \right)_{q,\beta} \quad d\epsilon_q^p = d\lambda \left( \frac{\partial f}{\partial q} \right)_{\sigma^B,\beta} \quad (52)$$

321 One of the simplest plastic model used for saturated clay is the Modified Cam-  
322 Clay model:

$$f_{\text{Cam}}(\sigma, q, p_0) = \sigma(\sigma + p_0) + q^2/M^2 \quad (53)$$

323 where  $p_0$  is the preconsolidation pressure at the saturated state which is gov-  
324 erned by the plastic void ratio:

$$p_0 = p_r \exp \left( -\frac{e^p}{\lambda(0) - \kappa} \right) \quad (54)$$

325 where  $\lambda(0)$  is the slope of the saturated virgin consolidation line while  $\kappa$  is the  
326 slope of the unloading/reloading line as introduced in section 4. A simple exten-  
327 sion of the yield function (53) to the unsaturated state can then be formulated  
328 as

$$f = f_{\text{Cam}}(\sigma^B, q, p_0) \quad (55)$$

329 where the preconsolidation pressure  $p_0$  should be extended to unsaturated sit-  
330 uations. Following the work of Coussy [13], we set

$$p_0 = p_r h(e^p, S_L) \quad (56)$$

331 where  $h$  should satisfy  $h(e^p, 1) = \exp \left( -\frac{e^p}{\lambda(0) - \kappa} \right)$ .

332 In the following we will assume that

$$h(e^p, S_L) = h_m(e^p) h_s(S_L) \quad (57)$$

333 where  $h_m = \exp \left( -\frac{e^p}{\lambda(0) - \kappa} \right)$  expresses the mechanical hardening due to irre-  
334 versible deformations and  $h_s$  represents a saturation-induced hardening (which

335 may be a function of capillary pressure through the retention curve). Note that  
 336  $h_s(1) = 1$ , leading to  $p_0 = p_r$  at the initial (undeformed) reference saturated  
 337 state.

## 338 5.1 Shear strength

339 Substitution of the Bishop effective stress (50) in the classical Mohr-Coulomb  
 340 criterion gives

$$\tau = C - (\sigma_n + \chi^p \pi_L + (1 - \chi^p) \pi_G) \tan \psi \quad (58)$$

341 where  $C$  is the cohesion and  $\psi$  is the friction angle which is assumed constant,  
 342 consistently with the Cam-Clay model:  $\sin \psi = 3M/(6 + M)$ . Alonso et al [3]  
 343 have shown that the coefficient  $\chi^p$  to consider in the shear strength of unsat-  
 344 urated soils is actually smaller than the saturation degree. They proposed a  
 345 generic formula of the form

$$\chi^p = \left\langle \frac{S_L - S_L^m}{1 - S_L^m} \right\rangle \quad (59)$$

346 where  $\langle x \rangle = (x + |x|)/2$  is the positive part operator. Alonso et al related  
 347 this coefficient (called effective degree of saturation in their paper) to the freely  
 348 available water filling the macroporosity of the soil. Here we will rather use  
 349 this formula as a parametric form of the coefficient  $\chi^p$ . From (20) and (14), a  
 350 development of Eq. (58) in terms of the capillary pressure,  $p_c = p_G - p_L$ , and  
 351 interface energy,  $U$ , gives

$$\tau = C - \left( \sigma_n + p_G - \chi^p p_c - \frac{2}{3} \left( -\frac{\chi^p}{S_L} a + \frac{1 - \chi^p}{1 - S_L} (1 + a) \right) U \right) \tan \psi \quad (60)$$

352 Numerous experiments have been performed on shear strength of unsaturated  
353 soils. We present in the figure (3) those performed on Guadalix de la Sierra red  
354 clay [16] for which  $C = 0$  and  $\psi = 33^\circ$ . In the same figure we have plotted the  
355 model as predicted by Eq. (60) under different hypotheses:  $\chi^p = S_L$  or  $\chi^p$  given  
356 by Eq. (59). The model of Brooks and Corey [8] was used to fit the retention  
357 curve with an air entry pressure of 30 kPa and an exponent equal to 3.

## 358 5.2 Isotropic stress path at constant capillary pressure

359 The compression index of a normally consolidated saturated soil is defined by

$$de = -\lambda(0) \frac{d(\sigma + p)}{\sigma + p} \quad (61)$$

360 For an unsaturated soil at constant capillary pressure, an isotropic plastic load-  
361 ing on the virgin compression line, i.e  $-\sigma^B = p_0$ , results in

$$de^p = -(\lambda(0) - \kappa) \frac{d\sigma^B}{\sigma^B} \quad (62)$$

362 Assuming that  $\chi = \chi^p$  entails

$$de = -\lambda(0) \frac{d\sigma^B}{\sigma^B} \quad (63)$$

363 which is the simplest extension of (61) for unsaturated situations. We assume  
364 moreover, hereafter, that  $\chi = \chi^p = S_L$ . We have applied this simple model to  
365 a silty clay [25, 26, 35]. The figure (4b) reports the variation of the void ratio  
366 during a compression oedometric test from 1 to 256 kPa obtained at different  
367 capillary pressures:  $p_c = 0, 20, 40, 80, 160$  kPa. The figure (4a) shows the predic-  
368 tion obtained by the model. The elastic limit, given by  $-\sigma = \pi + p_0$ , has been

369 identified to 18, 22, 24, 28, 50 kPa respectively. From these results we have iden-  
370 tified the following parameters associated to the saturated state:  $\lambda(0) = 0.037$ ,  
371  $\kappa = 0,004$  and  $p_r = 18$  kPa. To assess the value of the interface energy,  $U$ ,  
372 we use a retention curve fitted by using the model of Brooks and Corey with  
373 the parameters associated to the silty clay (air entry pressure  $p_e = 10$  kPa and  
374 exponent  $\alpha = 2.5$ ).

### 375 **5.3 Imbibition drainage paths**

376 The same silty clay as that used in the previous section was loaded at differ-  
377 ent isotropic compression stresses:  $-\sigma = 8, 16, 32, 64, 128, 256$  kPa. After each  
378 compression test, the capillary pressure is increased from 0 to 160 kPa then the  
379 specimen is unloaded to its initial compression, i.e 1 kPa. The same parameters  
380 as those defined in the last section are used. Figure (5a) shows the void ratio  
381 variations during the different loading paths. The vertical lines correspond to  
382 the capillary pressure load. The corresponding evolution of the void ratio is  
383 represented in the figure (6a). The experimental results are represented in the  
384 figures (5b) and (6b).

385 Let's consider now a soil sample initially and normally saturated. The initial  
386 capillary pressure is equal to zero. Let's submit the specimen to increasing  
387 capillary pressure from 1 to 256 kPa. The capillary pressure is then decreased  
388 to 1 kPa. We use the following parameters  $\lambda(0) = 0.19$ ,  $\kappa = 0.031$ ,  $p_r = 10$  kPa,  
389 and an initial stress  $-\sigma_0 = 1.5 \cdot 10^{-6}$  kPa. The parameters of the retention curve  
390 (Brook and Corey) are given by  $p_e = 1.8$  MPa and  $\alpha = 1$ . These parameters

391 correspond to a white clay used in [17]. The experiments are shown in the  
 392 figure (7b) and can be compared to the predictions shown in the figure (7a). In  
 393 the experiment the sample is not mechanically loaded. So we found the initial  
 394 stress in order to fit one point of the curve. We found the very small value  $-\sigma_0 =$   
 395  $1.5 \cdot 10^{-6}$  kPa. During the loading path from 1 to 1.8 kPa the capillary pressure is  
 396 lower than the air entry pressure and the soil is actually saturated. The slope of  
 397 the curve is the compression index. For capillary pressure greater than 1.8 kPa  
 398 the sample behaves elastically because we assumed that the saturation-induced  
 399 hardening  $h_s(S_L) > 1 + \frac{\chi^p p_e - p_e}{p_r h_m(e^p)}$ , resulting in a strictly negative yield function:  
 400  $f < 0$ .

## 401 6 Conclusion

402 The model proposed by Coussy [13] has been extended to account for interface  
 403 energies in the mechanical behaviour of unsaturated soils. This extension relies  
 404 on the assumption that the interface energy depends on the partial pore defor-  
 405 mations in addition to the saturation degree. As a consequence, effective pore  
 406 pressures should be considered in the mechanical behaviour in place of the liquid  
 407 and gas pressures. These effective pore pressures differ from the pore pressures  
 408 by terms involving the interface energy. Following the approach developed in  
 409 Coussy et al, a Bishop-like effective stress, expressed in terms of these effective  
 410 pore pressures, is found to control the mechanical behaviour of unsaturated soils  
 411 providing an assumption concerning the partial pore deformations, i.e the de-

412 formation of the partial volume occupied by the fluids. The Bishop's coefficient,  
413  $\chi$ , turns out to be a saturation dependent fraction of the partial pore deforma-  
414 tion and the total pore deformation. Actually two Bishop-like effective stresses,  
415 associated to the elastic and plastic behaviour, can be introduced. This results  
416 in a model relying on two effective stresses which can be used to extend the  
417 elastic and plastic behaviour of saturated soils to unsaturated conditions. We  
418 propose a very simple model based on the extension of the Cam-Clay model.  
419 This model is applied to predict the response of a soil sample to compression  
420 stress at constant capillary pressure and to wetting drying paths at constant  
421 stress. These responses are compared with some experimental results reported  
422 from the literature.

## 423 **References**

- 424 [1] G.D. Aitchison. Separate roles of site investigation, quantification of soil  
425 properties and selection of operational environment in the determination  
426 of foundation design on expansive soils. In *Proc 3rd Asian Regional Conf.*  
427 *Soil Mech. Found. Engng*, volume 3, pages 72–77, Haifa, Israel, 1967.
- 428 [2] E.E. Alonso, A. Gens, and A. Josa. A constitutive model for partially  
429 saturated soils. *Géotechnique*, 30:504–430, 1990.
- 430 [3] E.E. Alonso, J.M. Prereira, J. Vaunat, and S. Olivella. A microstructurally  
431 based effective stress for unsaturated soils. *Géotechnique*, 60(12):913–925,  
432 2010.



- 433 [4] A. W. Bishop. The principle of effective stress. *Teknisk Ukeblad*, 39:859–  
434 863, 1959.
- 435 [5] A. W. Bishop and G.E. Blight. Some aspects of effective stress in saturated  
436 and partly saturated soils. *Géotechnique*, 13 (1):177–197, 1963.
- 437 [6] G.E. Blight. A study of effective stress for volume change. In G.D. Aitchi-  
438 son, editor, *Moisture equilibria and moisture changes in soils beneath cov-  
439 ered areas*, pages 259–269, Sydney, 1965. Butterworths.
- 440 [7] G. Bolzon, B.A. Schrefler, and O.C. Zienkiewicz. Elastoplastic soil constitu-  
441 tive laws generalized to partially saturated states. *Géotechnique*, 13(3):279–  
442 289, 1996.
- 443 [8] R.N. Brooks and A.T. Corey. Hydraulic properties of porous media. *Col-  
444 orado State Univ. Hydrol. Paper*, 3:270–278, 1964.
- 445 [9] J.B. Burland. Some aspects of the mechanical behaviour of partially sat-  
446 urated soils. *Moisture Equilibria and Moisture Changes Beneath Covered  
447 Areas*, pages 270–278, 1965.
- 448 [10] X. Chateau and L. Dormieux. Micromechanics of saturated and un sat-  
449 urated porous media. *International Journal of Numerical and Analytical  
450 Methods in Geomechanics*, 26:831–844, 2002.
- 451 [11] O. Coussy. *Poromechanics*. J. Wiley, 2004.

- 452 [12] O. Coussy. Revisiting the constitutive equations of unsaturated porous  
453 solids using a lagrangian saturation concept. *Int. J. Numer. Anal. Method*,  
454 31:1675–1694, 2007.
- 455 [13] O. Coussy, J.M. Pereira, and J. Vaunat. Revisiting the thermodynamics  
456 of hardening plasticity for unsaturated soils. *Computers and Geotechnics*,  
457 37:207–215, 2010.
- 458 [14] P. Dangla, O. Coussy, E. Olchitzky, and C. Imbert. Non linear thermo-  
459 mechanical couplings in unsaturated clay barriers. In W. Ehlers, editor,  
460 *Theoretical and numerical methods in continuum mechanics of porous ma-*  
461 *terials. Proceedings of IUTAM Symposium*. Kluwer Academic Publishers,  
462 2000.
- 463 [15] W. Ehlers, T. Graf, and M. Ammann. Deformation and localizaton analysis  
464 of partially saturated soil. *Comput. Methods Appl. Mech. Engng.*, 193(27-  
465 29):2885–2910, 2004.
- 466 [16] V. Escario. Formulaciones para la difinicion de la resistencia a esfuerzo  
467 cortante de los suelos parcialmente saturados. *Ingeniera Civil*, 68, 1988.
- 468 [17] J. M. Fleureau, S. Kheirbek-Saoud, R. Soemitro, and S. Taibi. Behavior  
469 of clayey soils on drying-wetting paths. *Canadian Geotechnical Journal*,  
470 30:287–296, 1993.
- 471 [18] D.G. Fredlund and N.R. Morgenstern. Stress state variables for unsaturated  
472 soils. *J. of Geot. Eng. Div., ASCE*, 103 (GT5):447–466, 1977.

- 473 [19] D. Gallipoli, A. Gens, R. Sharma, and J. Vaunat. An elastoplastic model for  
474 unsaturated soil incorporating the effects of suction and degree of saturation  
475 on mechanical behaviour. *Géotechnique*, 53(1):123–135, 2003.
- 476 [20] A. Gens and E.E. Alonso. A framework for the behaviour of unsaturated  
477 expansive clays. *Can. Geotech. J.*, 29(6):761–773, 1992.
- 478 [21] W.G. Gray and B.A. Schrefler. Thermodynamic approach to effective stress  
479 in partially saturated porous media. *Eur. J. Mech. A/Solids*, 20:521–538,  
480 2001.
- 481 [22] W.G. Gray and B.A. Schrefler. Analysis of the solid phase stress tensor in  
482 multiphase porous media. *Int. J. Numer. Anal. Meth. Geomech.*, 31:541–  
483 581, 2007.
- 484 [23] J.E.B. Jennings and J.B. Burland. Limitations to the use of effective  
485 stresses in partly saturated soils. *Géotechnique*, 12:125–144, 1964.
- 486 [24] Y. Khogo, M. Nakano, and T. Miyazaki. Theoretical aspects of constitutive  
487 modelling for unsaturated soils. *Soils Found.*, 33(4):49–63, 1993.
- 488 [25] J. Leclercq and J.C. Verbrugge. Considérations relatives à la mécanique  
489 des sols non saturés et à son intérêt en agronomie. *Bulletin de Recherches*  
490 *Agronomiques*, 19:237–267, 1984.
- 491 [26] J. Leclercq and J.C. Verbrugge. Propriétés géomécaniques des sols non  
492 saturés. In *Colloque International "Le travail du sol"*, pages 1–15, Gem-  
493 bloux le 29/11/1985, Faculté Universitaire des sciences agronomiques, 1985.

- 494 [27] R.W. Lewis and B.A. Schrefler. *The finite element method in static and*  
495 *dynamic deformation and consolidation of porous media*. John Wiley &  
496 Sons, 1998.
- 497 [28] B. Loret and N. Khalili. A three-phase model for unsaturated soils. *Int. J.*  
498 *Numer. Anal. Methods Geomech.*, 24:893–927, 2000.
- 499 [29] B. Loret and N. Khalili. An effective stress elastic-plastic model for unsat-  
500 urated porous media. *Mech. Mater.*, 34:97–116, 2002.
- 501 [30] A. Modaressi and N. Abou-Bekr. Constitutive model for unsaturated soils:  
502 validation on a silty material. In *Proc. Numer. Methods Geomechan., NU-*  
503 *MOG V*, volume 1, pages 91–96, 1994.
- 504 [31] M. Nuth and L. Laloui. Effective stress concept in saturated soils: Clarifi-  
505 cation and validation of a unified framework. *Int. J. Numer. Anal. Meth.*  
506 *Geomech.*, 32:771–801, 2008.
- 507 [32] J.M. Pereira, H. Wong, P. Dubujet, and P. Dangla. Adaptation of existing  
508 behaviour models to unsaturated states: application to cjs model. *Inter-*  
509 *national Journal for Numerical and Analytical Methods in Geomechanics*,  
510 29:1127–1155, 2005.
- 511 [33] R. Santagiuliana and B.A. Schrefler. Enhancing the bolzon-schrefler-  
512 zienkiewicz constitutive model for partially saturated soil. *Trans. Porous*  
513 *Media*, 65(1):1–30, 2006.

- 514 [34] D. Sheng, S.W. Sloan, and A. Gens. A constitutive model for unsatu-  
515 rated soils: thermomechanical and computational aspects. *Comput. Mech.*,  
516 33(6):453–465, 2004.
- 517 [35] S. Taibi. *Comportement mécanique et hydraulique des sols partiellement*  
518 *saturés*. PhD thesis, Ecole Central de Paris, 1994.
- 519 [36] S.J. Wheeler, R.S. Sharma, and M.S.R. Buisson. Coupling of hydraulic  
520 hysteresis and stress-strain behaviour in unsaturated soils. *Géotechnique*,  
521 53(1):41–54, 2003.

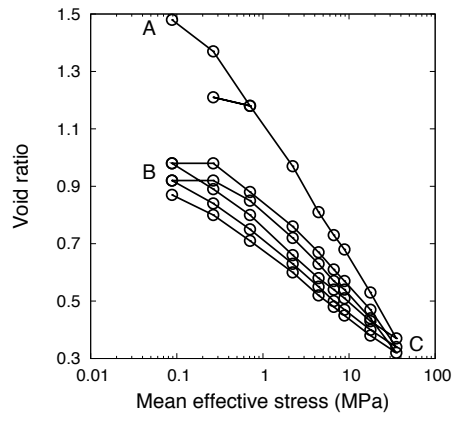


Figure 1: Isotropic compression test performed on saturated FoCa clay [14].

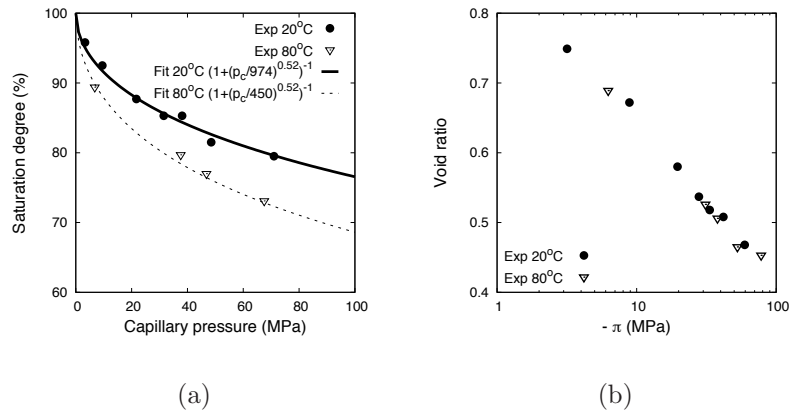
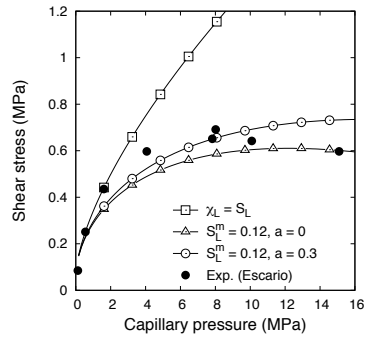
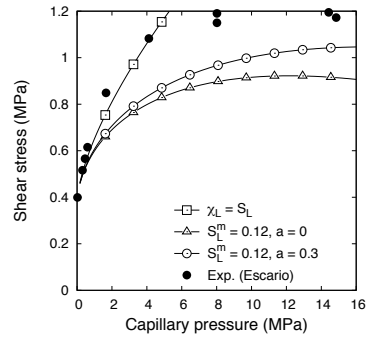


Figure 2: (a) Retention curve of a FoCa clay obtained by saturated salt solution technique [14]. (b) Void ratio reported against  $\log(-\pi)$  in a free swelling during imbibition test.



(a)



(b)

Figure 3: Shear strength vs capillary pressure obtained at different normal stress: (a) 0.12 MPa (b) 0.6 MPa. The experimental results are reported from Escario et al [16].



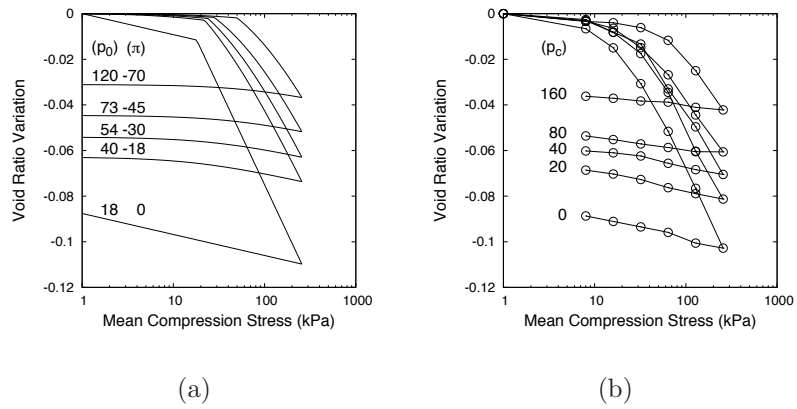
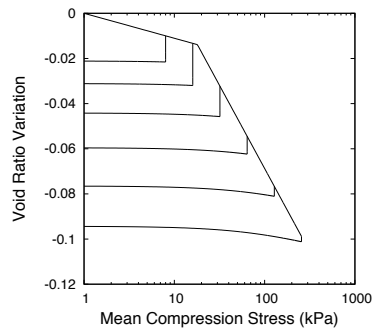
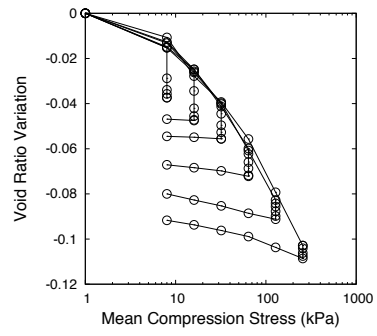


Figure 4: Isotropic compression curves at constant capillary pressure obtained on a silty clay: (a) Model (b) Experiment reported from [25, 26].

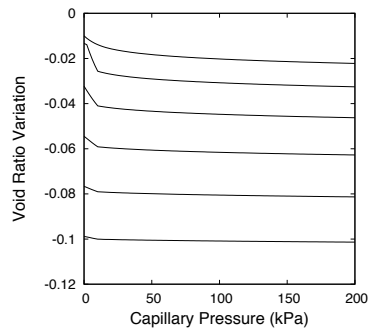


(a)

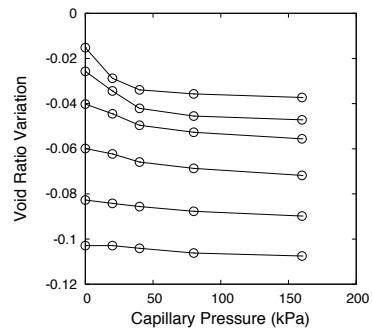


(b)

Figure 5: Compression, drainage and unloading on a silty clay: (a) model (b) experiments [25, 26].

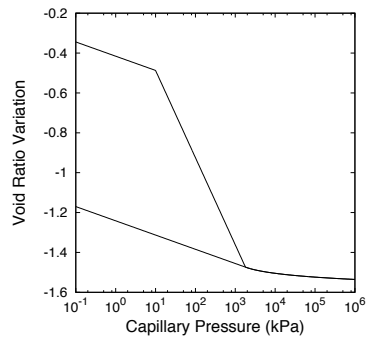


(a)

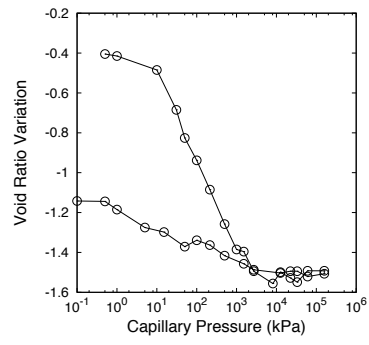


(b)

Figure 6: Drainage phase on a silty clay: (a) model (b) experiments [25, 26].



(a)



(b)

Figure 7: Drainage on a white clay: (a) model (b) experiments [17].